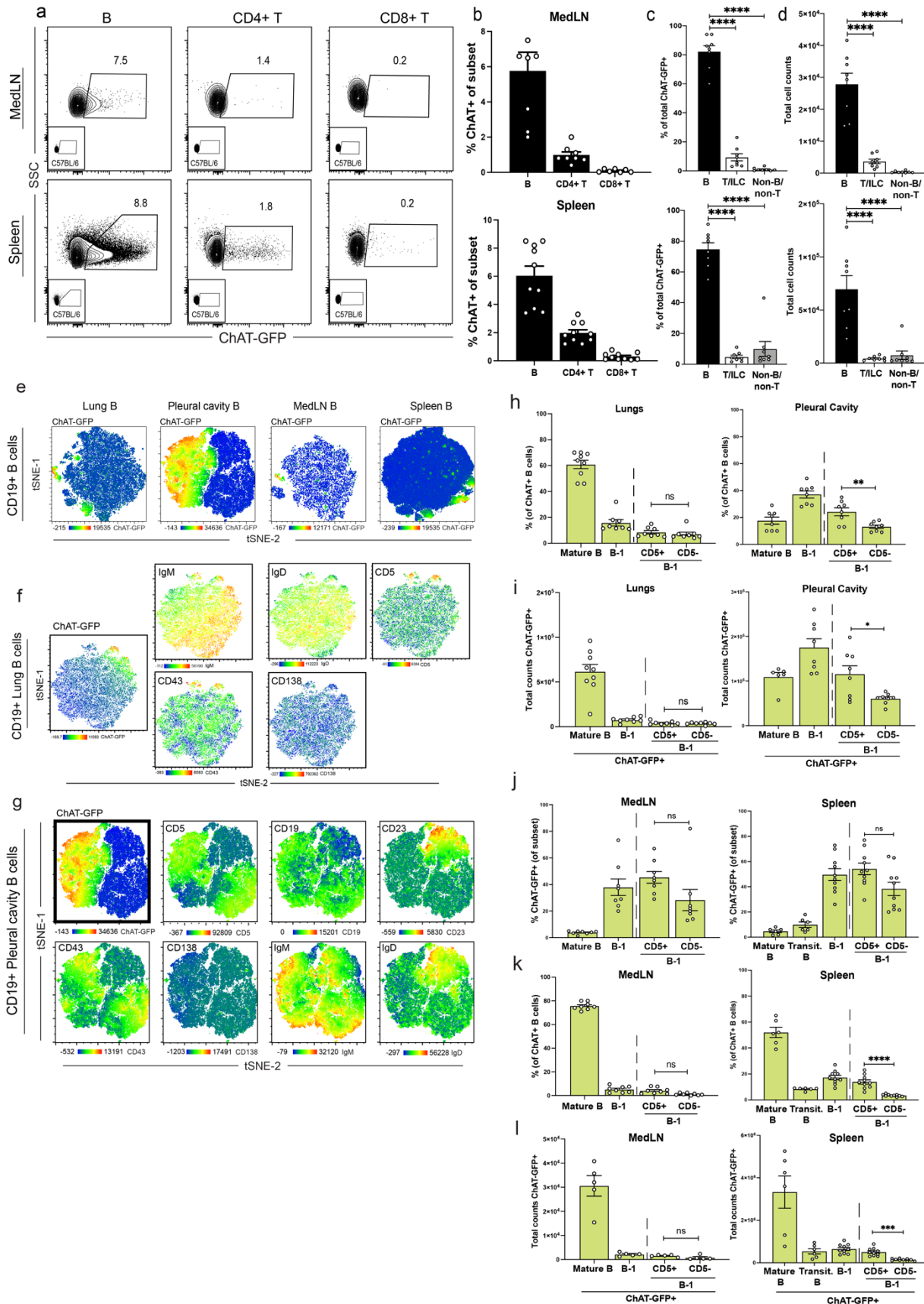
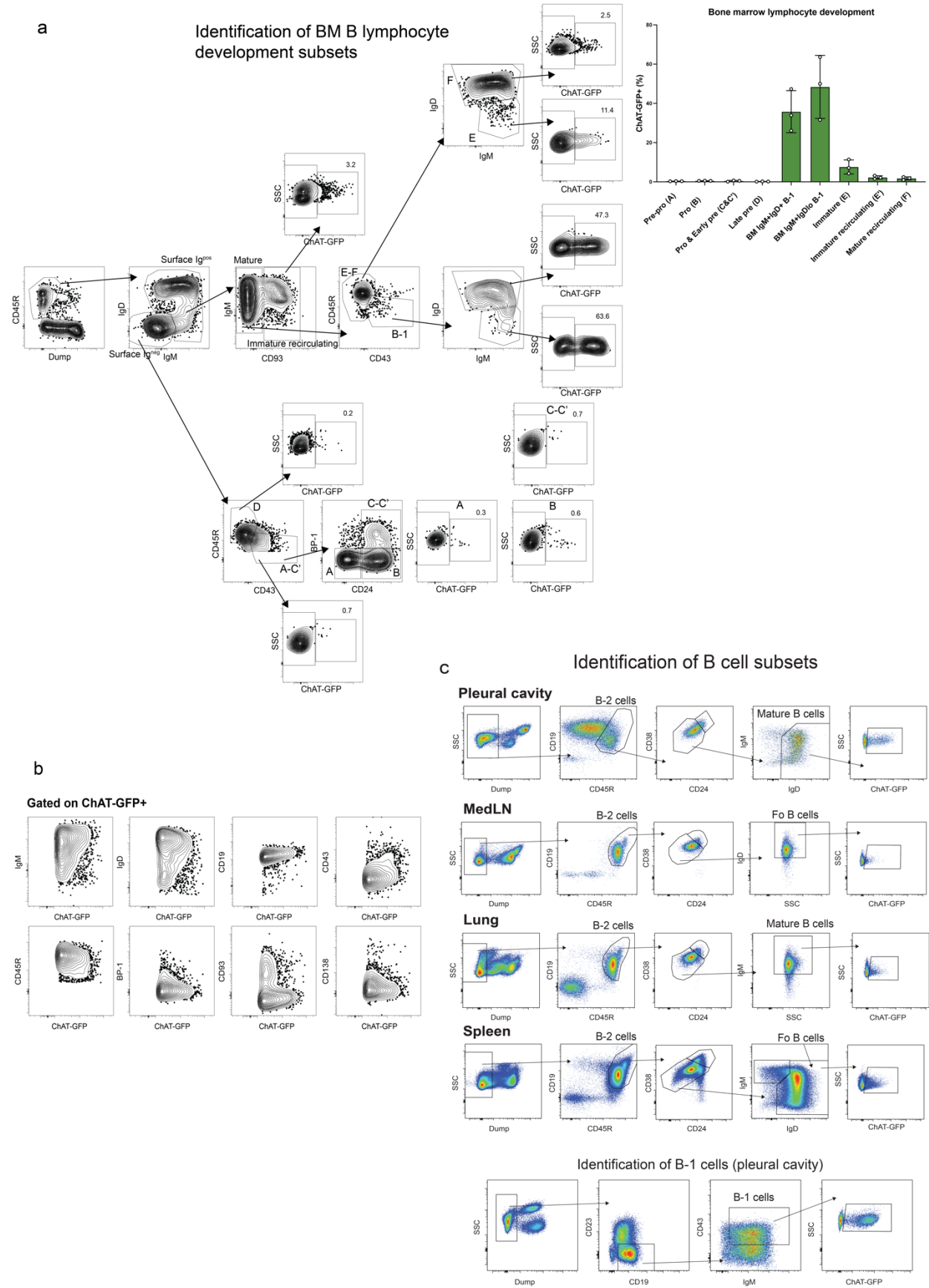


**Extended Data Fig. 1. ACh inhibits pro-inflammatory cytokine production including TNF- $\alpha$ , induced after influenza infection in lung interstitial macrophages (IMs).** a) C57BL/6 mice (n=4-6/group) were infected with indicated plaque-forming units (PFU) of influenza A/PR8 on d0 for 10-15 days. Shown is the mean percentage weight change + SD over the course of the infection compared to d0. b) C57BL/6 mice (n = 4-6) were infected with indicated doses of influenza A/PR8 i.n. and lungs were analyzed by flow cytometry at 1 day post infection. Shown are representative flow cytometry plots (left) and MFI of TNF $\alpha$ -expression among lung total macrophages (right) gated on CD19-, Thy1.2-, Ly6G-, Ly6C-, F4/80+/CD64+ (top), alveolar macrophages (AMs) further gated on CD11b-, CD11c+, SiglecF+ (middle), or interstitial macrophages (IMs) further gated on CD11b+, CD11c-, SiglecF- (bottom) after ex-vivo restimulation with LPS in the presence of Brefeldin A for 4h at 37°C. a) n=4-6/group mice pooled from 2 independent experiments. b) Results were pooled from 2 independent experiments. Bar graphs show mean  $\pm$  s.e.m. Symbols indicate results from an individual mouse. One-Way ANOVA. \*p<0.05; \*\*p<0.01; \*\*\*p<0.001; \*\*\*\*p<0.0001; n.s. not significant.



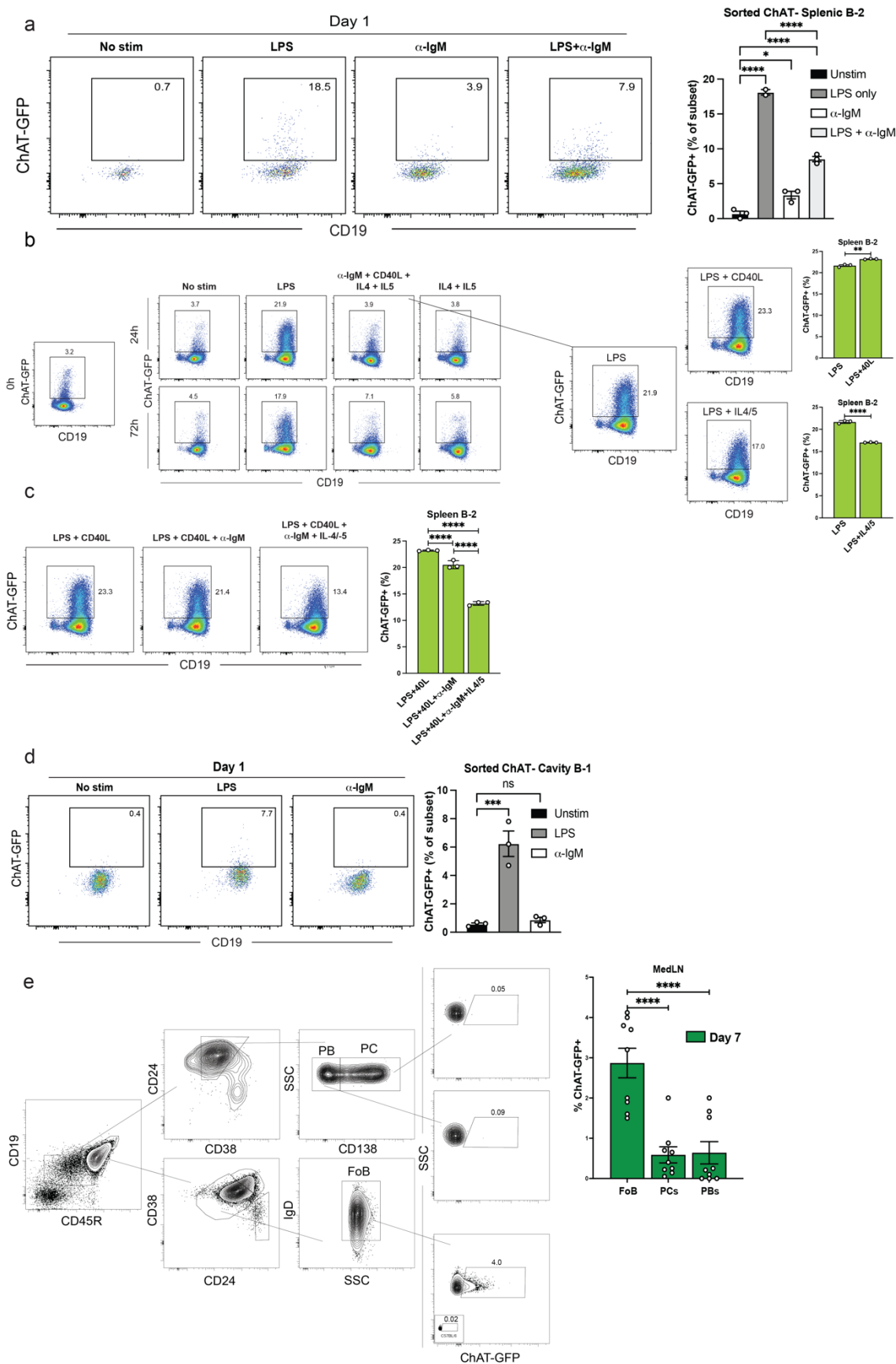
**Extended Data Figure 2. B cells are the major ChAT-expressing leukocytes at steady state.** a) representative flow cytometry plots for the identification of ChAT-GFP+ B, CD4+ and CD8+ T cells from mediastinal lymph node (MedLN) (top) and spleen (bottom) of GFP-ChAT reporter mice. Small inserts show same populations from non-GFP expressing C57BL/6 mice. b) summary of ChAT-GFP+ frequencies among CD19+ B cells, CD3+ CD4+ and CD3+ CD8+ T cells in the MedLN (top) and spleen (bottom). c) frequencies of ChAT-GFP+ cells that are either B (CD19+), T/ILC (CD3+ or CD90.2+) or Non-B/Non-T (CD19- CD3-, CD90.2-). d) cell counts of ChAT-GFP+ B, T/ILC and Non-B/Non-T cells in the MedLN (top) and spleen (bottom). e) tSNE plots with heat map indicating ChAT-GFP expression of B cells (CD19+, Thy1.2-) from indicated tissues (lungs, pleural cavity, MedLN and Spleen). f) flow cytometry tSNE plots of lung B cells (CD19+, Thy1.2-) with heat map quantifying expression of indicated surface markers. g) flow cytometry tSNE plots of pleural cavity B cells (CD19+, Thy1.2-) with heat map quantifying expression of indicated surface markers h) summary of ChAT-GFP+ frequencies of B cell subsets (gating strategy, **Extended Data Figure 2**) among total ChAT-GFP+ B cells (CD19+, Thy1.2-) in the lung and pleural cavity. i) cell counts of ChAT-GFP+ B cell subsets in the lungs and pleural cavity. j) frequencies of ChAT-GFP+ cells among B cell subsets in the MedLN and spleen. k) frequency of ChAT-GFP+ frequencies of B cell subsets among total ChAT-GFP+ B cells (CD19+, Thy1.2-) in the MedLN and spleen. l) cell counts of ChAT-GFP+ B cell subsets in the MedLN and spleen. a-d) n=6-9 mice pooled from 3 independent experiments. e-g) representative of 2 independent experiments with n=3 mice per tissue. h-l) n=6-9 mice pooled from 3 independent experiments. Bar graphs indicate mean  $\pm$  s.e.m. Symbols indicate results from an individual mouse; a-d) One-way ANOVA; h-l) two-tailed unpaired Student's t-test.

\*p<0.05; \*\*p<0.01; \*\*\*p<0.001; \*\*\*\*p<0.0001; n.s. not significant.

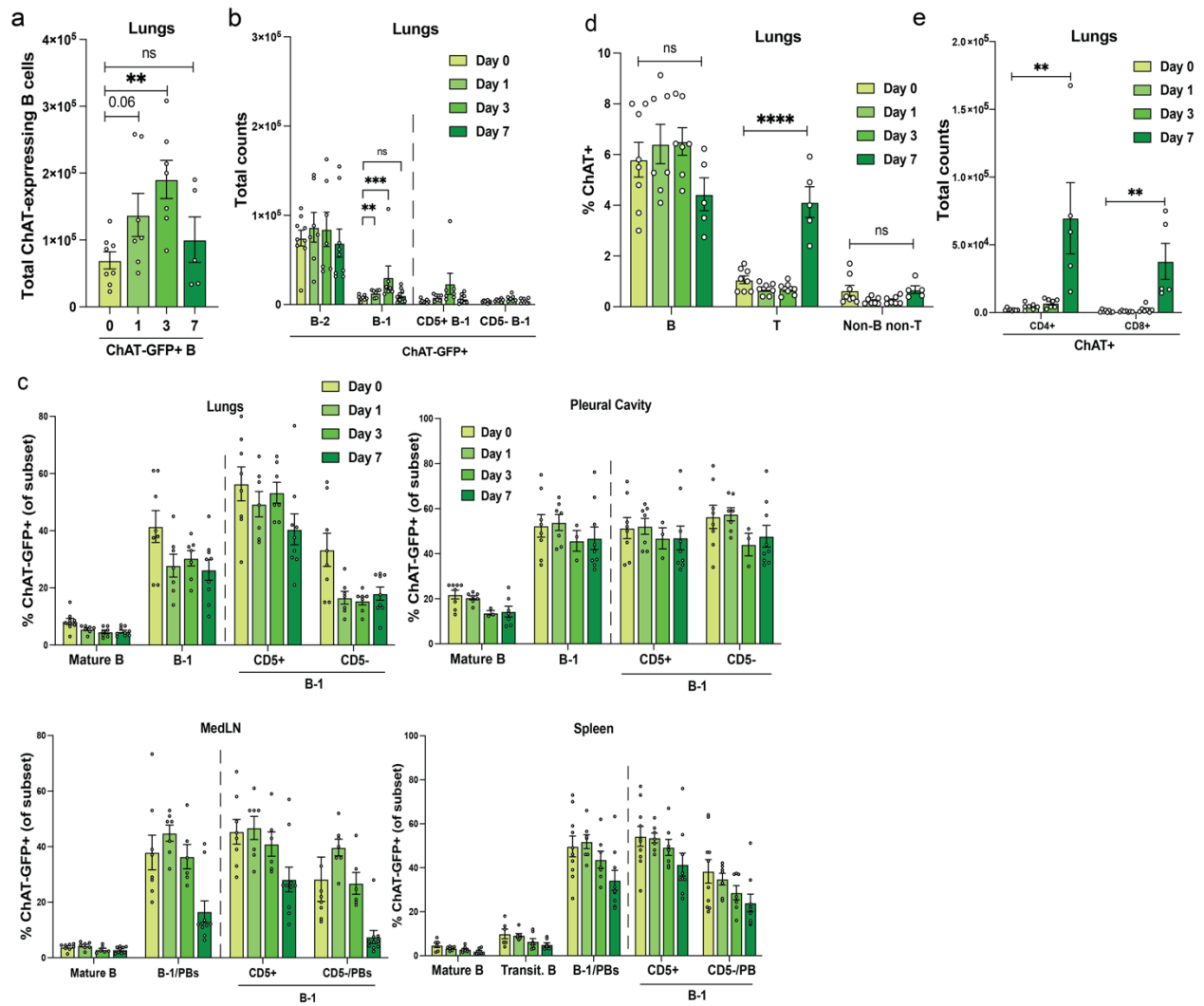


**Extended Data Figure 3. ChAT induction first occurs at the immature B cell stage.** a, b)

Bone Marrow (BM) was harvested from ChAT-GFP reporter mice (n=3) and analyzed by flow cytometry using an amended Hardy Scheme gating strategy to identify ChAT-expression among B cell differentiation stages. **a)** (left) gating strategy using CD45R to identify B cells and separation of cells into surface Ig+ and Ig negative cells (lower panels), which were then divided into CD43+ (Hardy Fr. A-C') and CD43- (Hardy Fr. D). Surface Ig+ cells were divided into CD93 (immature, Hardy Fr. E) and CD93- cells. The latter were further separated into CD43- mature circulating B cells (Hardy Fr. F), and CD43+ IgMhi IgDlo B-1 cells; (right) quantification of BM ChAT-GFP+ B cells as frequency of the indicated B cell subset. **b)** representative flow plots showing the relationship between ChAT-GFP expression and other surface markers used to define B cell developmental stages. **c)** gating strategy to identify different B cell subsets in all tissues analyzed (lungs, pleural cavity, mediastinal lymph nodes and spleen). Results in a) are representative of 2 independent experiments with n=3 mice each. Bar graphs show mean  $\pm$  s.e.m. Symbols indicate results from an individual mouse. \*p<0.05; \*\*p<0.01; \*\*\*p<0.001; \*\*\*\*p<0.0001; n.s. not significant.

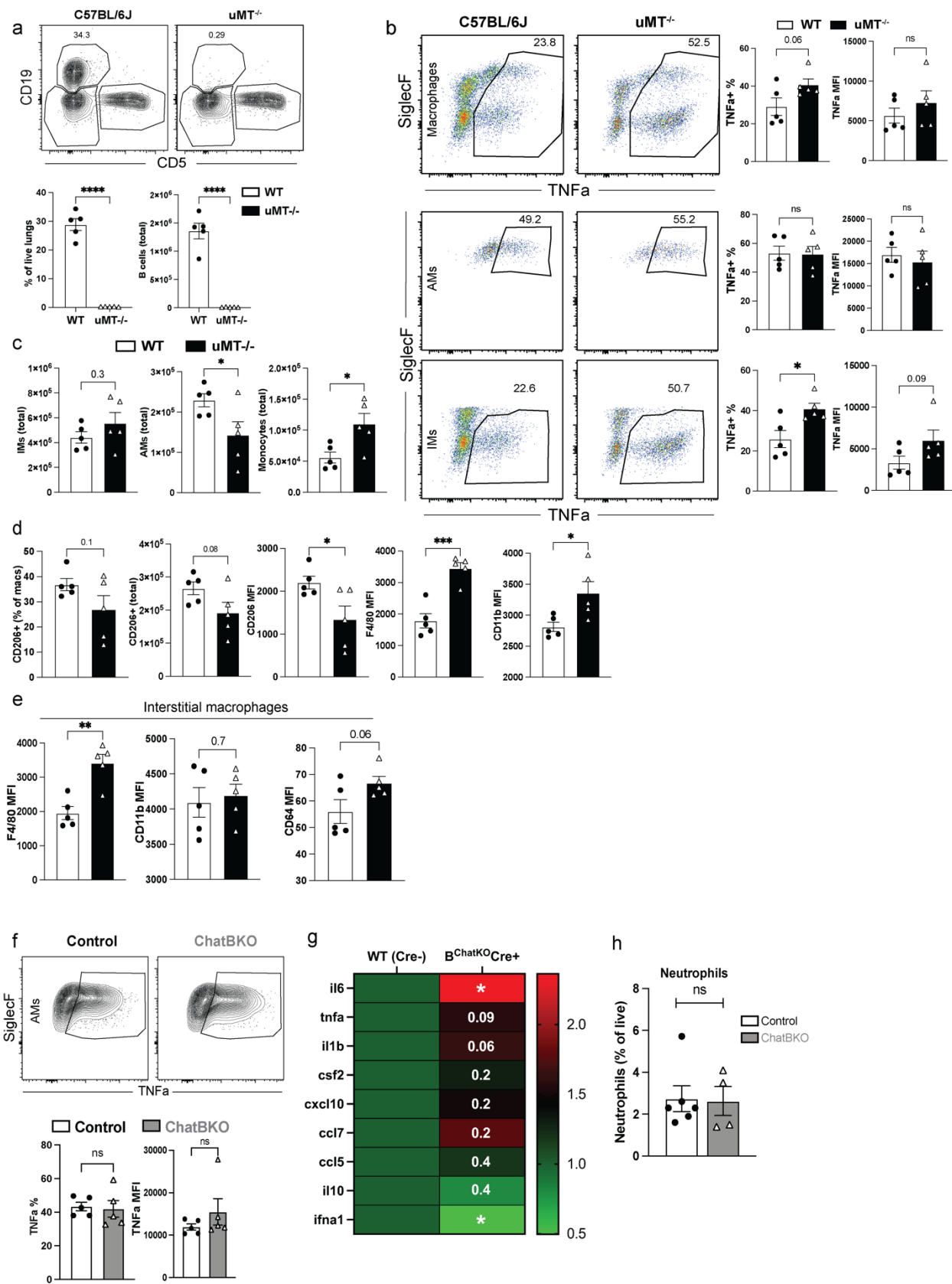


**Extended Data Figure 4. ChAT induction signals in B cells.** a-d) representative flow cytometry plots (left) and frequencies (right) of ChAT-GFP expression among (a) FACS-sorted splenic ChAT-GFP<sup>neg</sup> B-2 cells (CD19+, CD23+, CD43-, CD5-, CD9-, ChAT-GFP<sup>neg</sup>) or (b-d) magnetically-enriched total splenic B-2 cells (CD19+, CD23+, CD43-, CD5-, CD9-) from ChAT-GFP reporter mice cultured in the presence or absence of LPS, anti-IgM (Fab)<sub>2</sub>, or indicated stimuli, for indicated times. d) representative flow cytometry plots (left) and frequencies (right) of ChAT-GFP expressing FACS-sorted pleural cavity ChAT-GFP<sup>neg</sup> B-1 cells (CD19+, CD23-, CD43+, ChAT-GFP<sup>neg</sup>) cultured in the presence or absence of LPS, anti-IgM (Fab)<sub>2</sub>, or both, for 24h. e) ChAT-GFP reporter mice were infected intranasally (i.n.) with 10PFU A/PR8 for 7 days. Draining mediastinal lymph nodes (MedLN) were analyzed by flow cytometry; representative flow cytometry plots and gating strategy (left) and frequencies (right) of ChAT-GFP expressing Follicular B cells (FoB), Plasmablasts (PB) or plasma cells (PC). a-d) representative of 2 experiments with similar results; data represent n=3 total replicates per group e) n=6-10 mice, pooled from 3 independent experiments. Bar graphs indicate mean  $\pm$  s.e.m. a-e) One-Way ANOVA \*p<0.05; \*\*p<0.01; \*\*\*p<0.001; \*\*\*\*p<0.0001; n.s. not significant.

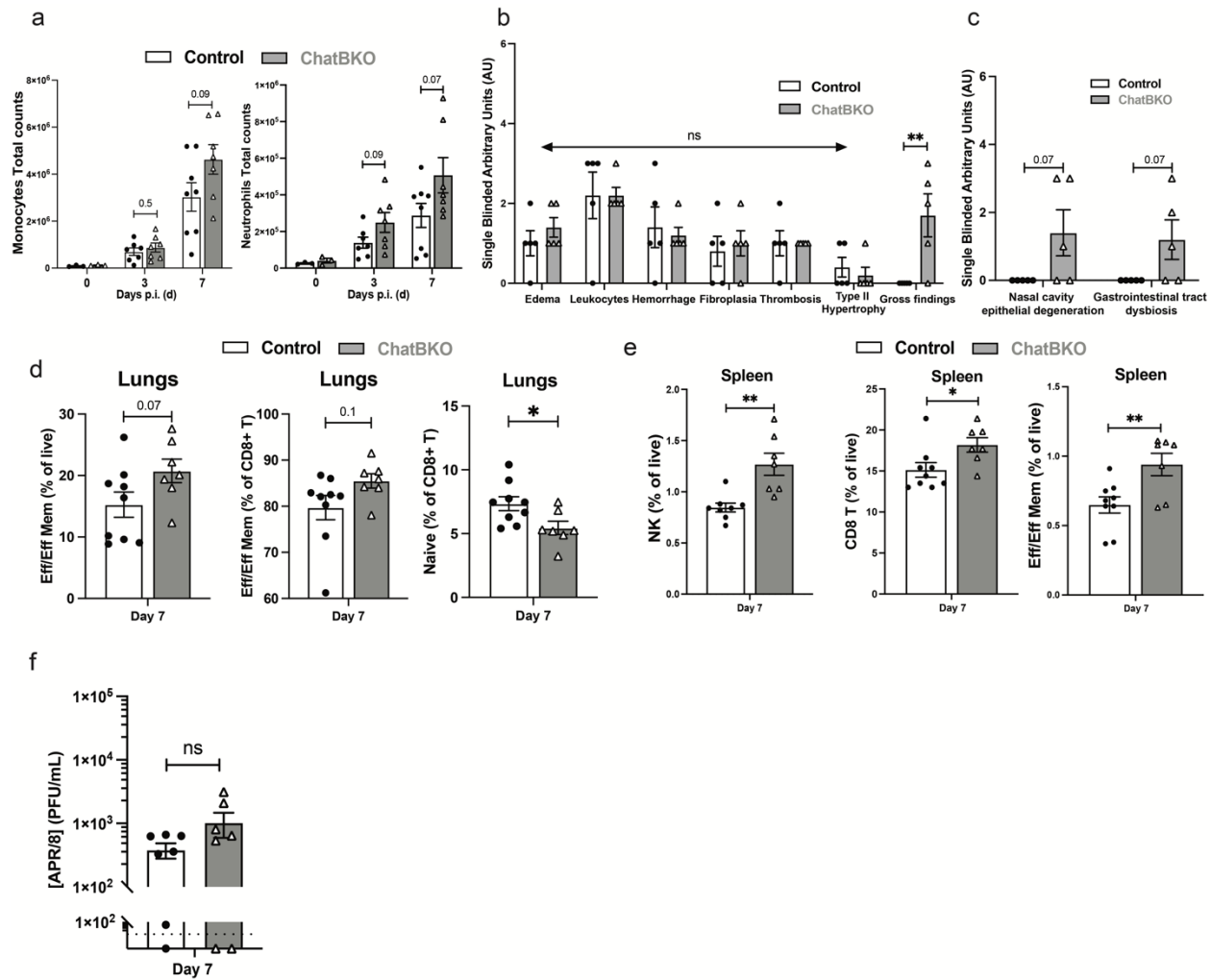


***Extended Data Figure 5. ChAT B cell induction and redistribution after influenza infection***

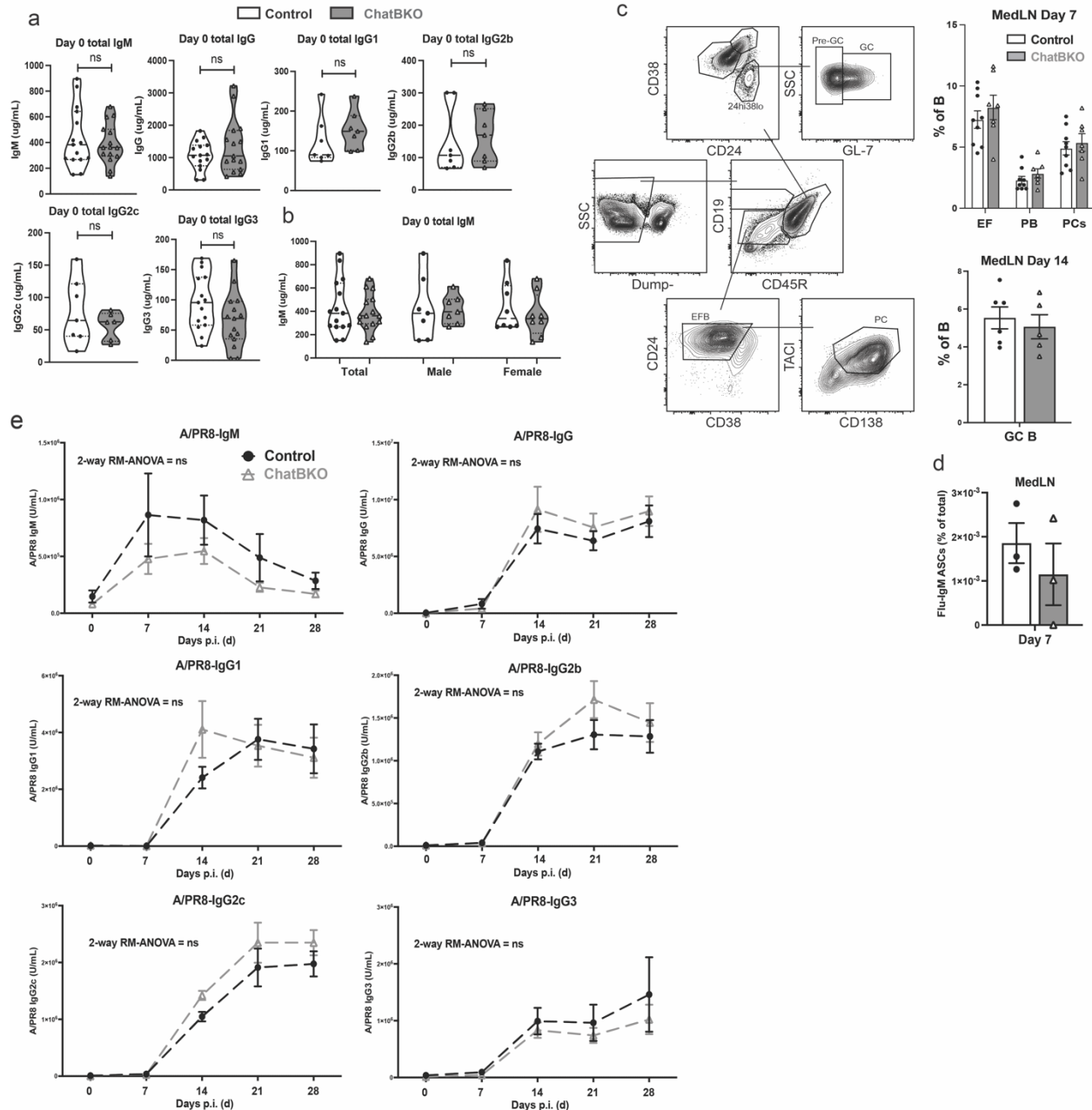
a-d) ChAT-GFP reporter mice were infected with 10PFU A/PR8 and the lungs, pleural cavity, mediastinal lymph nodes (MedLN) and spleen were analyzed via flow cytometry on 0, 1, 3 and 7 days post infection (dpi). b) total cell counts of ChAT-GFP+ B cells (left) or of ChAT-GFP B cell subsets (***Extended Data Figure 2c***) (right), at indicated dpi with influenza. c) frequency of ChAT-GFP+ expressing cells among each B cell subset in lungs, pleural cavity, spleen and MedLN d) frequency of ChAT-GFP+ B (CD19+), T-ILC (CD3+ or Thy1.2+) and Non-B/Non-T (CD19-, CD3-, Thy1.2-) among total ChAT-GFP+ cells. e) cell counts of ChAT-GFP+ CD4+ and CD8+ T cells in the lungs at indicated days after influenza infection. a-e) n=6-10 mice, pooled from 3 independent experiments. Bar graphs show mean  $\pm$  s.e.m. Symbols indicate results from an individual mouse. b-e) One-Way ANOVA. \*p<0.05; \*\*p<0.01; \*\*\*p<0.001; \*\*\*\*p<0.0001; n.s. not significant.



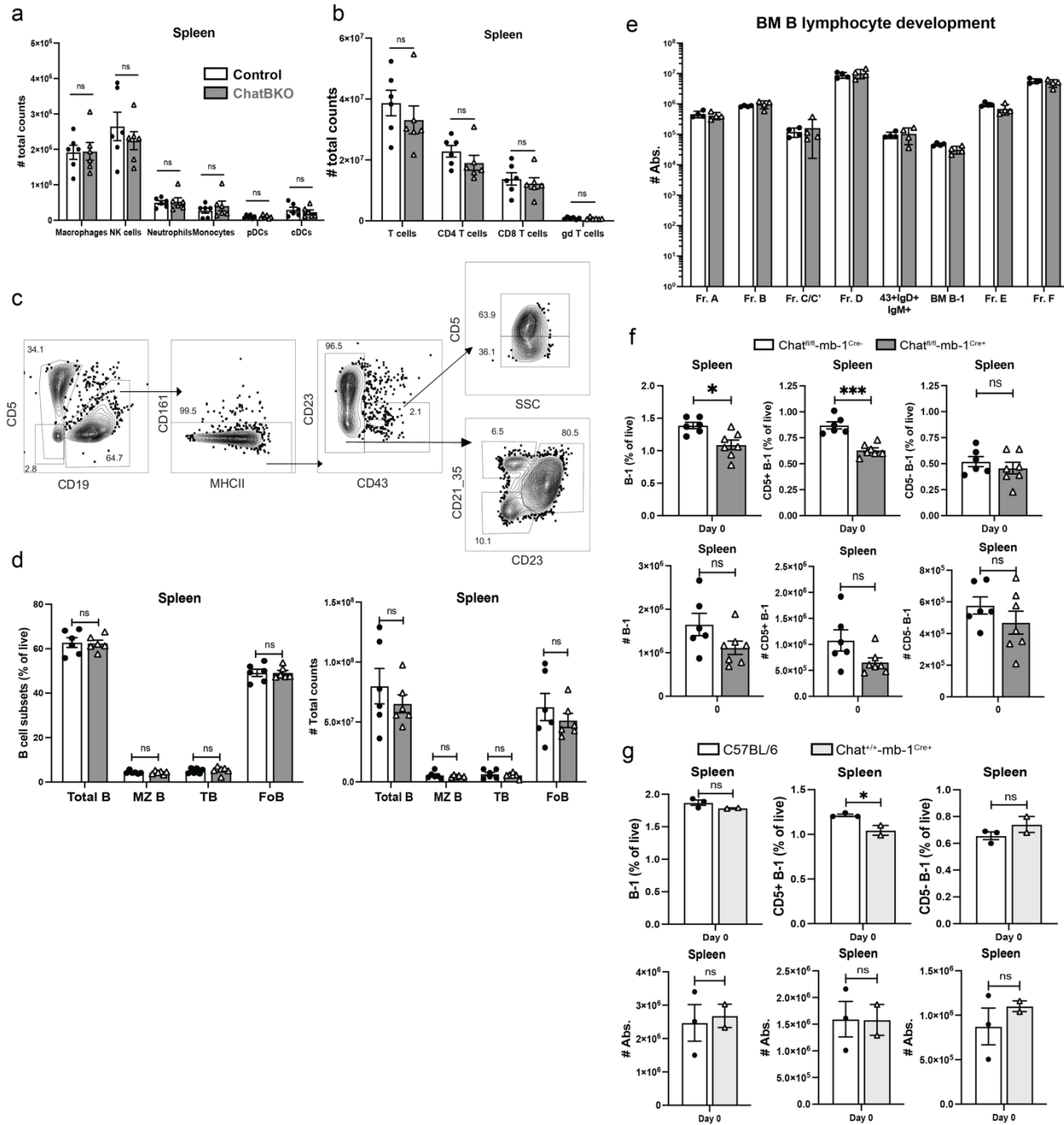
**Extended Data Figure 6. B cells control lung interstitial macrophage responses via ACh.** a) representative flow cytometry plots (top) and frequencies (bottom) of B cells (CD19+, CD5-) in the lungs of WT C57BL/6 and uMT-/- mice. b-e) WT C57BL/6 and uMT-/- mice (n=4-6) were infected with 10PFU A/PR8 i.n. and lungs were analyzed via flow cytometry at day 1 post-infection. b) representative flow cytometry plots (left) and frequencies and MFI (right and far right, respectively) of TNF $\alpha$ -expressing lung total macrophages (top; CD19-, ThY1.2-, Ly6G-, Ly6C-, F4/80+/CD64+), alveolar macrophages (AMs; middle; further gated on CD11b-, CD11c+, SiglecF+), and interstitial macrophages (IMs; bottom; further gated on CD11b+, CD11c-, SiglecF) after ex-vivo restimulation with LPS in the presence of Brefeldin A for 4h at 37°C. c) total counts of lung IMs (left), AMs (middle) or monocytes (right) gated as in (b). d) frequencies and total numbers of lung parenchyma CD206+ macrophages and MFI of indicated markers among total macrophages and (e) of IMs only, as assessed by flow cytometry. f-h) mb-1Cre $^{+/-}$  ChAT $^{fl/fl}$  (Control) and mb-1Cre $^{+/-}$  ChAT $^{fl/fl}$  (ChatBKO) mice were infected with 10PFU A/PR8 i.n. and lungs were analyzed at 1 dpi. f) representative flow plots (top) and frequencies (bottom) of TNF $\alpha$ -expressing lung alveolar macrophages (AMs) gated as in (b), after ex-vivo restimulation with LPS in the presence of Brefeldin A for 4h at 37°C. g) Relative gene expression of indicated cytokine and chemokines in lung homogenates from Control and ChatBKO mice at 1dpi. h) frequency of lung neutrophils (CD19-, Thy1.2-, Ly6C-, Ly6G+) at 1dpi in Control and ChatBKO mice (n=5). a-h) n=4-6 mice pooled from 2 independent experiments. Bar graphs show mean  $\pm$  s.e.m. Symbols indicate results from an individual mouse a-h) two-tailed unpaired Student's t-test \*p<0.05; \*\*p<0.01; \*\*\*p<0.001; \*\*\*\*p<0.0001; n.s. not significant.



**Extended data Figure 7. The absence of B cell-derived ACh leads to increased innate immune cell recruitment into the lung, and to systemic inflammation.** a) Lung homogenates from mb-1Cre<sup>-/-</sup> ChAT<sup>fl/fl</sup> (Control) and mb-1Cre<sup>+/+</sup> ChAT<sup>fl/fl</sup> (ChatBKO) mice (n=6-8) infected with 10PFU A/PR8 were analyzed via flow cytometry at 0, 3 and 7 days post-infection (dpi). a) total cell counts of monocytes (CD19-, Thy1.2-, Ly6G-, Ly6C+) and neutrophils (CD19-, Thy1.2-, Ly6C-, Ly6G+). b-c) Control and ChatBKO mice (n=5) were infected with 100PFU A/PR8 and lungs and gut content were analyzed at 7 dpi. B, c) Arbitrary units of disease score for lung histology, nasal cavity epithelial cells and gastrointestinal tract for indicated parameters. d-e) Control and ChatBKO mice (n=7-10) were infected i.n. with 100PFU A/PR8 and lungs and spleens were analyzed via flow cytometry at 7dpi. d) frequencies of effector memory CD8+ T cells cells (CD3+, CD4-, CD8+, CD44hi, CD62L-) and Naïve CD8+ T cells (CD3+, CD4-, CD8+, CD44lo, CD62L+) among live cells, or CD8+ T cells. e) frequencies of NK cells (left; CD19-, Th1.2-, Ly6G-, Ly6C-, NK1.1+), CD8+ T cells (middle) and Effector/Effector Memory CD8+ T cells (right). f) Influenza A viral loads in lung homogenates at 1dpi (n=6-8/group) assessed by qRT-PCR. a, d-f) n=6-10 mice pooled from 3 independent experiments; b, c) n=5 mice; g) n = 4-6 mice per group. Bar graphs show mean  $\pm$  s.e.m. Symbols indicate results from an individual mouse. a-f) two-tailed unpaired Student's t-test. \*p<0.05; \*\*p<0.01; \*\*\*p<0.001; \*\*\*\*p<0.0001; n.s. not significant.

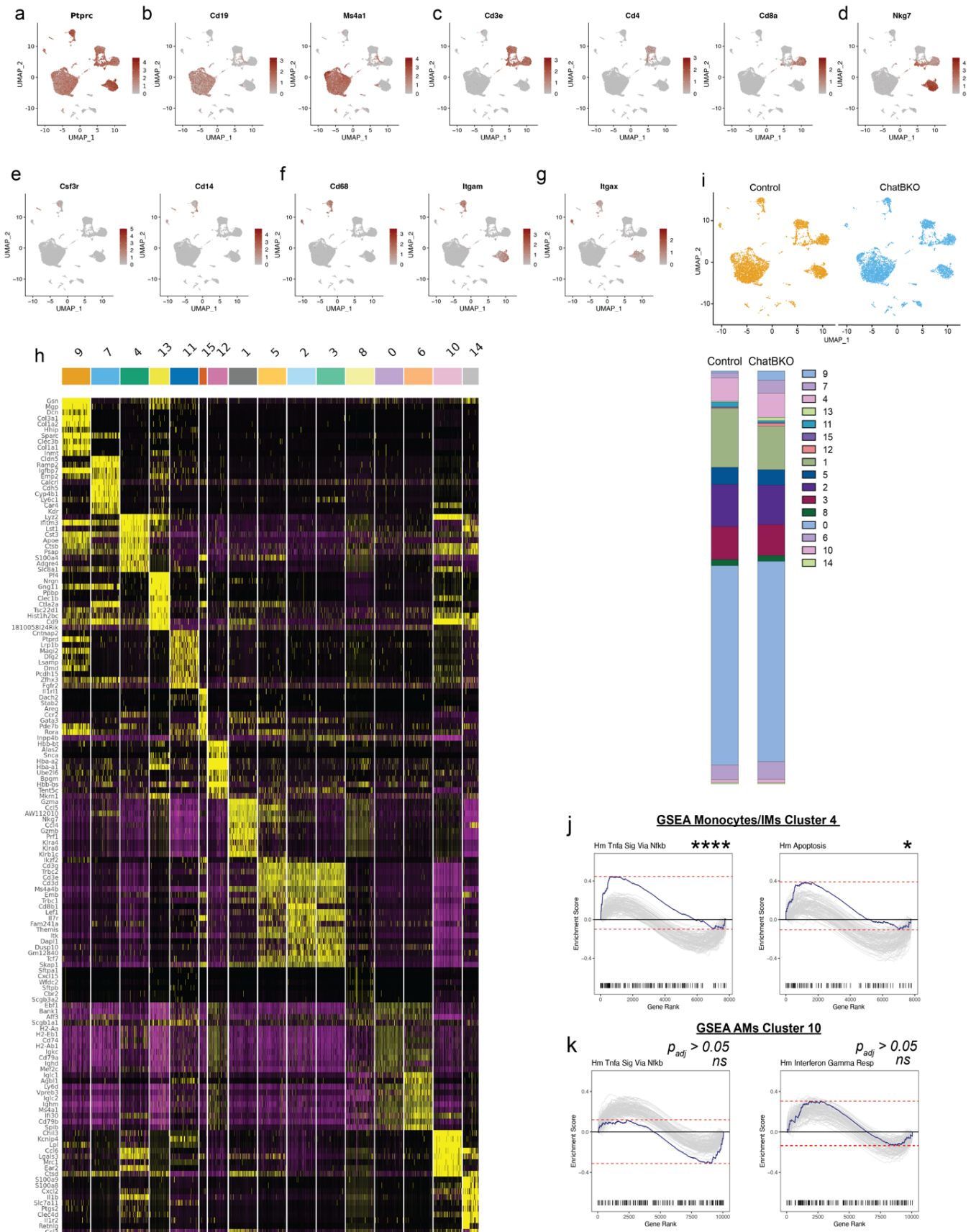


**Extended Data Figure 8. B cell-derived ACh does not affect antibody production.** **a)** Serum IgM, IgG, IgG1, IgG2b and IgG2c concentrations in non-infected mb-1Cre<sup>-/-</sup> ChAT<sup>fl/fl</sup> (Control) and mb-1Cre<sup>+/+</sup> ChAT<sup>fl/fl</sup> (ChatBKO) mice (n=8-14/group) and **b)** total concentration of serum IgM comparing male and female mice in Control and ChatBKO mice by ELISA. **c)** Representative flow cytometry plots of mediastinal lymph nodes (MedLN) from Control and ChatBKO mice infected intranasally (i.n.) with 10PFU A/PR8 for 7 days (left), and frequencies of Extrafollicular B cells (EF), Plasmablasts (PB) or plasma cells (PC) at 7dpi (top-right) and frequencies of Germinal Center B cells (GC B) at 14dpi (bottom-right). **d)** A/PR8-specific IgM ASCs in the MedLN at 7dpi as measured by ELISPOT. **e)** Influenza specific serum IgM, IgG, IgG1, IgG2b, IgG2c, IgG3 in Control and ChatBKO mice (n=8-10/group) infected i.n. with 10PFU A/PR8 assessed by ELISA. a, b) Mice pooled from 3 independent experiments c) n=6-8 mice, pooled from 3 independent experiments. d) representative of 2 independent experiments with n=3 which gave similar results. e) results from n=8-10 mice/group pooled from 2 independent experiments. Bar graphs and violin plots show mean  $\pm$  s.e.m. Symbols indicate results from an individual mouse. a-d) two-tailed unpaired Student's t-test. e) repeated measure 2-way ANOVA. \*p<0.05; \*\*p<0.01; \*\*\*p<0.001; \*\*\*\*p<0.0001; n.s. not significant.

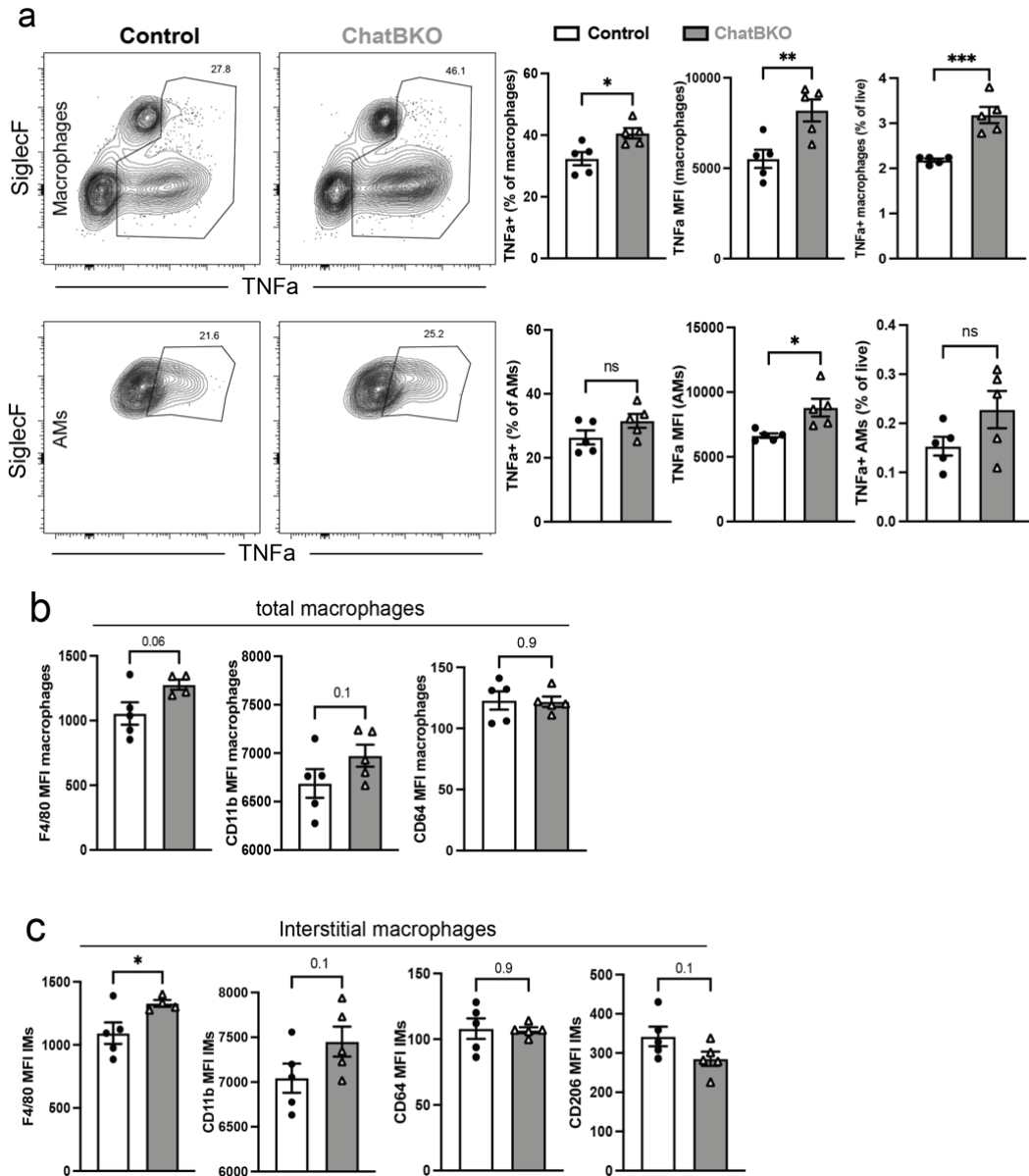


**Extended Data Figure 9. Lack of B cell-express ChAT does not affect steady state leukocyte composition nor B cell development.** **a-e)** flow cytometric analysis of adult male and female mb-1Cre<sup>-/-</sup> ChAT<sup>fl/fl</sup> (Control) and mb-1Cre<sup>+/+</sup> ChAT<sup>fl/fl</sup> (ChatBKO) mice. **a, b)** cell counts of (a) innate leukocytes, and (b) T cells. **c)** flow cytometric gating strategy to identify B cell subsets in the spleen. **d)** frequency and absolute numbers of B cell subsets in spleen steady state comparing Control and ChatBKO mice. **e)** Bone Marrow (BM) B lymphocyte development subsets using the Hardy gating scheme as in (Extended Data Fig. 2). **f)** frequencies (top) and total numbers (bottom) of B-1 cells and CD5+ and CD5- B-1 cells comparing Control and ChatBKO mice. **g)** similar to (f) but comparing C57BL/6 and mb-1Cre<sup>+/+</sup> ChAT<sup>+/+</sup> mice. **a-d, f)** n=6-8 mice pooled from 2 independent experiments. **e, g)** representative of 2 independent experiments with similar results, n=2-4 each. Bar graphs show mean  $\pm$  s.e.m. Symbols indicate results from an individual mouse. **a-g)** two-tailed unpaired Student's t-test.

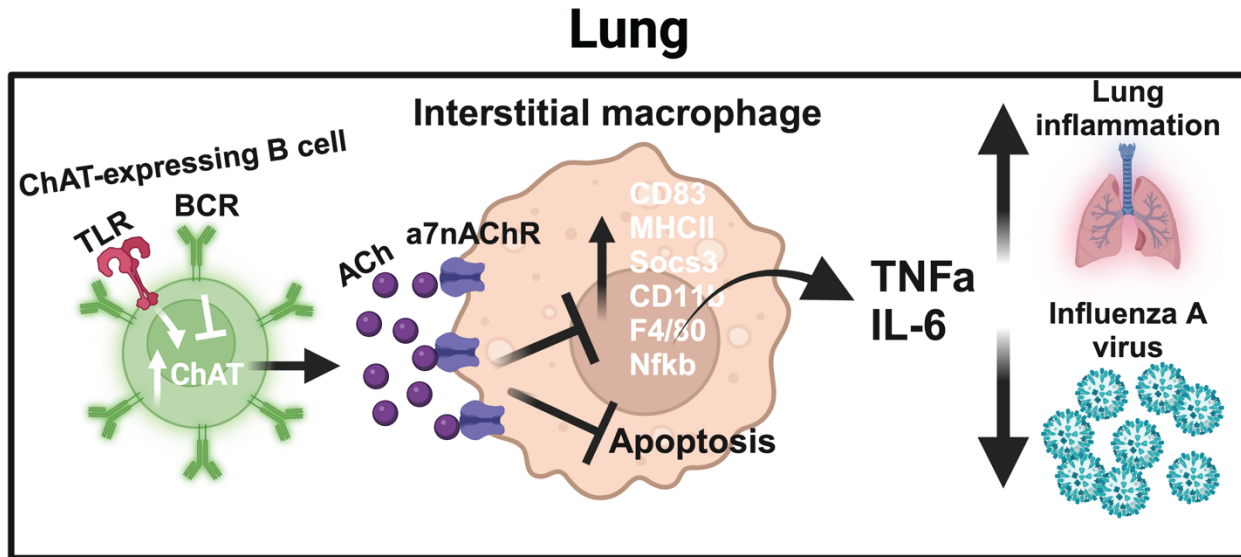
\*p<0.05; \*\*p<0.01; \*\*\*p<0.001; \*\*\*\*p<0.0001; n.s. not significant.



**Extended Data Fig. 10. scRNA-Seq data, supplementing Figure 3.** a-g) scRNA-Seq post-sample integration UMAP analysis plots from live, single cells of lungs from mb-1Cre<sup>-/-</sup> ChAT<sup>fl/fl</sup> (Control) and mb-1Cre<sup>+/+</sup> ChAT<sup>fl/fl</sup> (ChatBKO) mice (n=4 females/group) indicating expression levels of indicated canonical cell lineage markers. The intensity of expression is indicated by red coloring. h) Heat map of post-sample integration gene clustering analysis indicating the ten most differentially expressed genes across all clusters. i) (top) scRNA-Sequencing pre-sample integration UMAP plots of lung parenchyma cells from Control (orange) and ChATBKO (blue) mice, and (bottom) frequencies of cells by cluster and sample, compared to the total number of cells per sample plotted as a stacked bar chart. j) scRNA-Seq hallmark Tnfa Signaling via NfkB and apoptosis pathway analyses for cluster 4 (IMs) and k) hallmark Tnfa Signaling via NfkB and interferon gamma response pathways for cluster 10 (AMs). \*p<0.05; \*\*p<0.01; \*\*\*p<0.001; \*\*\*\*p<0.0001; n.s. not significant



**Extended Data Fig. 11. B cell derived ACh inhibits lung interstitial, but not alveolar, macrophage activation.** a-c) flow cytometry of single cell suspensions from lung parenchyma of mb-1Cre<sup>-/-</sup> ChAT<sup>fl/fl</sup> (Control) and mb-1Cre<sup>+/+</sup> ChAT<sup>fl/fl</sup> (ChatBKO) mice. a) representative flow cytometry plots (left) and frequencies (right) of TNF $\alpha$ -expressing lung macrophages (top; CD19-, ThY1.2-, Ly6G-, Ly6C-, F4/80+/CD64+) and alveolar macrophages (bottom; AMs; CD19-, ThY1.2-, Ly6G-, Ly6C-, F4/80+/CD64+ CD11c+, CD11b-, SiglecF+), frequencies are of previous gate (% of macrophages), TNF $\alpha$  shown as frequencies of live, MFI and as a frequency of macrophages, respectively, after ex-vivo LPS restimulation in the presence of Brefeldin A for 4h at 37C. b) MFI of indicated markers (F4/80, CD11b, CD64) in total macrophages and c) in IMs. a-c) n=4-6 mice pooled from 2 independent experiments with 2-3 mice each. Bar charts show mean  $\pm$  s.e.m. Symbols indicate results from an individual mouse. Two-tailed unpaired Student's t-test \*p<0.05; \*\*p<0.01; \*\*\*p<0.001; \*\*\*\*p<0.0001; n.s. not significant.



**Extended Data Figure 12. Model of B cell-derived control of interstitial macrophage inflammatory responses and viral loads via ACh.** Lung B cells, upon receiving innate-like signals such as TLR or TNFRSF, induce Choline Acetyltransferase (ChAT), enabling them to release Acetylcholine (ACh). In both steady-state conditions and immediately following influenza-infection, B cells engage with  $\alpha 7$  nicotinic Acetylcholine Receptor ( $\alpha 7nAChR$ )+ lung interstitial macrophages (IMs), residing in close proximity. B cell secretion of ACh stimulates IMs via  $\alpha 7nAChR$ , inhibiting apoptosis and suppressing local inflammation, thereby allowing enhanced early viral replication. This early-stage inhibition of pro-inflammatory cytokine production is beneficial to host organ function and local and systemic inflammation, helping the maintenance and/or repair of lung tissue during and after respiratory tract infection.